Dalton Transactions

Accepted Manuscript

This article can be cited before page numbers have been issued, to do this please use: R. Misra, T. Jadhav, B. Dhokale, P. Gautam, R. Sharma, R. Maragani and M. M. Shaikh, *Dalton Trans.*, 2014, DOI: 10.1039/C4DT00983E.

ROYAL SOCIETY OF CHEMISTRY

www.rsc.org/dalton

View Article Online
DOI: 10.1039/C4DT00983E

Carbazole-BODIPY conjugates: design, synthesis, structure and properties

Rajneesh Misra,* Thaksen Jadhav, Bhausaheb Dhokale, Prabhat Gautam, Rekha Sharma, Ramesh Maragani and Shaikh M. Mobin

Department of Chemistry, Indian Institute of Technology Indore, Indore 452 017, India.

*E-mail: rajneeshmisra@iiti.ac.in

Toc:

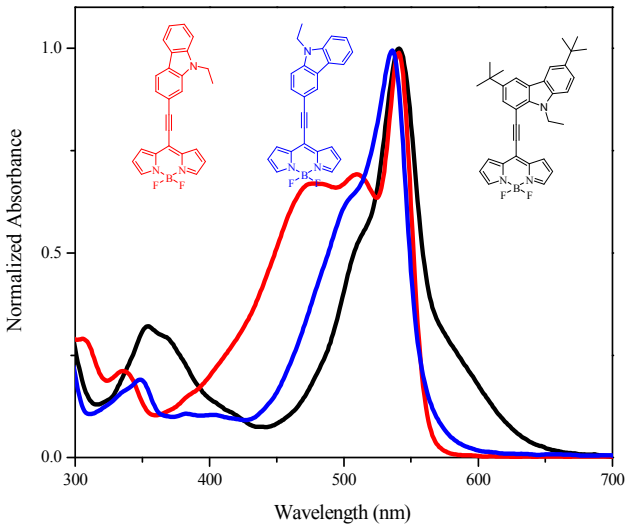

View Article Online
DOI: 10.1039/C4DT00983E

Abstract

A set of carbazole substituted BODIPYs **2a-2c** were designed and synthesized by the Pd-catalysed Sonogashira cross-coupling reaction. The effects of variation in the donor strength of various carbazoles were investigated by photophysical, electrochemical and computational studies. The electronic absorption spectra of BODIPYs **2a** and **2c** show charge transfer band, which show red shift in polar solvents. The BODIPYs **2a-2c** are highly fluorescent in nonpolar solvents (emission from localized state) and poorly fluorescent in polar solvents (emission from charge transfer state). The photophysical and electrochemical studies reveal strong donor-acceptor interaction between carbazole and BODIPY and follows the order **2a** > **2c** > **2b**. The computational calculations show good agreement with the experimental results. The single crystal structures of BODIPYs **2a-2c** are reported, which exhibits interesting supramolecular interactions. The packing diagram of **2a** show *zig zag* 3D structural arrangement, whereas **2b** and **2c** show complex 3D structural motifs.

Introduction

There has been continuous growing research interest in 4,4-difluoro-4-bora-3a,4a-diaza-s-indacene (BODIPY) dyes due to their strong acceptor nature and spectacular photophysical properties such as strong absorption with high extinction coefficient, high fluorescence quantum yield, and excellent photostability.[1] The BODIPY dyes have been explored in biochemical labeling, laser dyes, molecular electronics, photonics and electroluminescent materials.[2] Our group has explored the effect of various functional groups at the *β*-pyrrolic and *meso*-position of the BODIPY on its photophysical properties.[3] Recently, we have shown the quenching of fluorescence of the BODIPYs can be used as a measure of relative electron donating strength of

View Article Online
DOI: 10.1039/C4DT00983E

different aryl substituents.[4] In continuation of the our previous report, we were further interested to study the donor strength of different carbazoles.

Carbazole derivatives have been widely studied in optoelectronics due to its high chemical stability, low redox potential, hole transport property, and strong electron donating ability.[5] Nakamura and coworkers have explored the synthesis, and photophysical properties of thienylcarbazoles, and carbazole dimers.[6]

In order to study the electron releasing behavior of different carbazoles, we have connected it with *meso*-ethynyl-BODIPY. The electron releasing strength of the carbazole were found to be directly proportional to the photophysical properties of carbazole-BODIPY conjugates. It has been shown that the BODIPYs **2a-2c** show strong donor-acceptor interaction.

Results and Discussions

The BODIPYs **2a-2c** were synthesized by the Pd-catalyzed Sonogashira cross-coupling reaction of 8-chloro BODIPY **1** with respective ethynylcarbazoles **a-c** (Scheme 1). 8-chloro BODIPY **1**[7] and the ethynylcarbazoles[6,8] were synthesized by the reported procedures (Scheme S1).

The Sonogashira cross-coupling reaction of the 8-chloro BODIPY **1**, with the respective ethynylcarbazoles (**a-c)** at 0-5 °C in dichloromethane with $PdCl_2(PPh_3)_2$ as catalyst and CuI as co-catalyst resulted in BODIPYs **2a-2c** in 69%, 58% and 70% yields respectively. All the BODIPYs were well characterized by ^{1}H NMR, ^{13}C NMR, HR-MS and single crystal X-ray diffraction techniques. In the ^{1}H NMR spectrum of the BODIPYs, the β pyrrolic protons appear at the 6.5-6.6 ppm region, β' protons appear at 7.4-7.5 ppm region whereas the pair of two α protons appears at ~7.8 ppm (see supporting information).

View Article Online
DOI: 10.1039/C4DT00983E

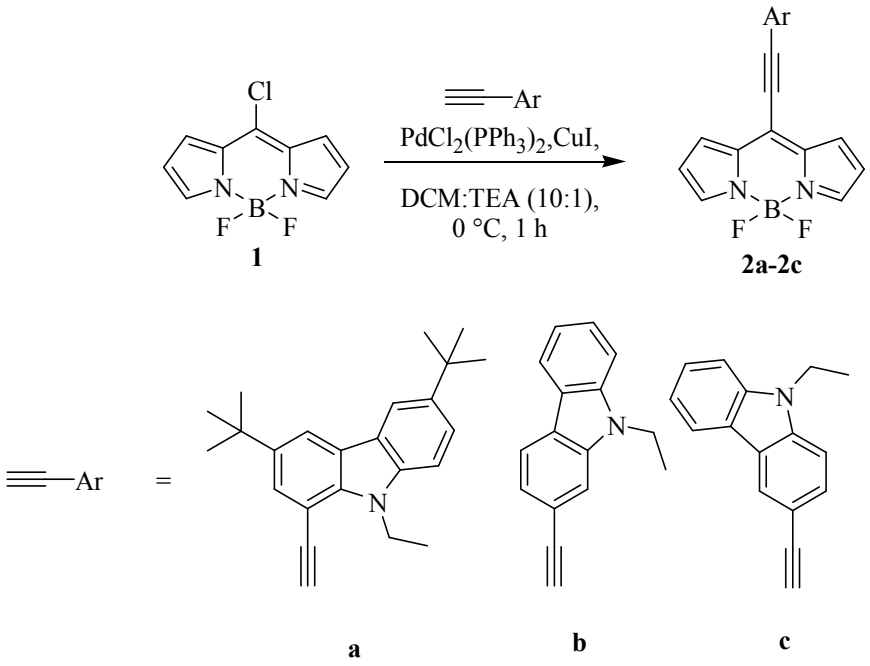

Scheme 1. Synthesis of BODIPYs **2a-2c.**

Thermal stability of the organic materials is key requirement for various optoelectronic applications. The thermal properties of BODIPYs **2a-2c** were investigated by the thermogravimetric analysis (TGA) at a heating rate of 10 °C min^{-1}, under nitrogen atmosphere (Fig. 1). The thermal decomposition temperature (T_d) for 10 % weight loss in the BODIPYs **2a-2c** was in the range of 320-368 °C (Table 1) and follows order **2c** > **2b** > **2a**. The presence of alkyl groups and steric hindrance lowers the thermal stability of BODIPY **2a**. The positional isomers **2b** and **2c** show similar thermal stability.

View Article Online
DOI: 10.1039/C4DT00983E

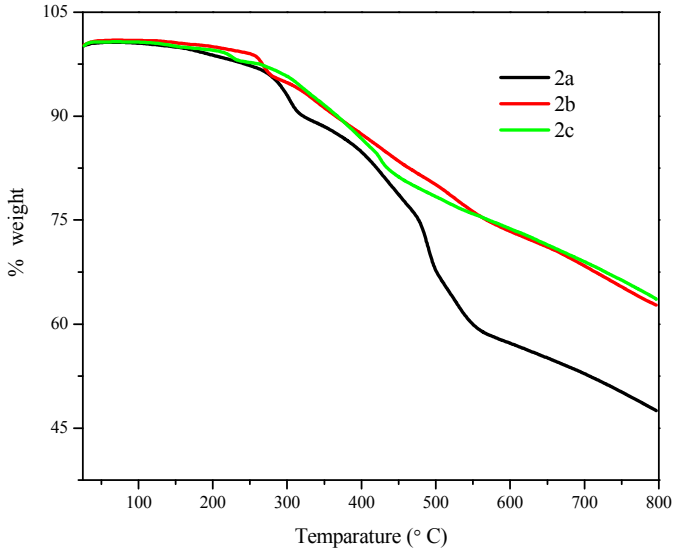

Fig. 1 TGA plots of the BODIPYs **2a-2c** at the heating rate of 10 °C min^{-1} under nitrogen atmosphere.

Photophysical Properties

The electronic absorption spectra of the BODIPYs **2a-2c** in different solvents are shown in Fig. 3 and the corresponding data are summarized in Table 1. The pictures of the BODIPYs **2a**–**2c** in toluene in day light and UV light are displayed in Fig. 2. The carbazole-BODIPY conjugates **2a-2c** show strong absorption band between 537–549 nm region with high extinction coefficient. The absorption spectrum in different solvents do not show significant effect on the band between 537–549 nm region, but show pronounced effect on the shoulder transitions in between 450-525 nm region. The BODIPY **2a** show charge transfer (CT) band at around 595 nm which was red shifted with increasing solvent polarity. This reflects strong donor-acceptor interaction between BODIPY and carbazole unit in BODIPY **2a**.[9,10] The BODIPY **2c** shows weak CT in polar solvents (tetrahydrofuran and dichloromethane) whereas CT band was absent in the case of **2b** irrespective of solvent polarity. The strength of CT band in BODIPYs **2a-2c** follows the order as **2a** > **2c** > **2b**.

View Article Online
DOI: 10.1039/C4DT00983E

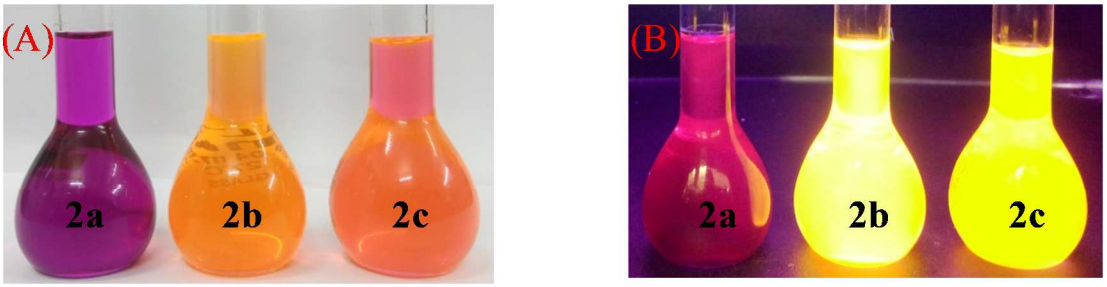

Fig. 2 The BODIPYs **2a**–**2c** in toluene at concentration of 10^{-4} M in day light (A) and in UV light (B).

Table 1. Photophysical and thermal properties of BODIPYs **2a-2c**.

BODIPY	solvent	λ_{abs}(nm)	$\varepsilon\times10^4$ (Mol^{-1}.cm^{-1})	λ_{em}[a] (nm)	Stokes Shift(cm^{-1})	ϕ_F[b]	T_d[c] (°C)	Optical band gap (eV)[d]	Theoretical band gap (eV)[e]
2a	Cyclohexane	544 513	5.79 2.85	583	1229	0.3537	322	2.11	2.59
	Toluene	547 516	5.98 3.01	671	3378	0.0564			
	THF	541 511	57.1 30.7	737	4916	0.0010			
	DCM	584 540 512	1.78 5.85 3.10	-	-				
2b	Cyclohexane	543 513 476	5.65 2.91 4.34	553	333	0.5512	366	2.21	2.80
	Toluene	547 514 477	5.32 3.09 3.62	562	488	0.4991			
	THF	541 510	4.91 3.41	556, 770	499	0.0031			
	DCM	541 511 481	5.40 3.83 3.61	-	-				
2c	Cyclohexane	539 500	8.28 7.81	548	304	0.3813	368	2.23	2.84
	Toluene	541 509	7.89 5.65	558	563	0.2252			
	THF	537 506	8.35 5.37	668	365	0.0030			
	DCM	537 504	7.55 4.64	-	-				

[a]Excitation at λ_{max}, [b]Determined by using Rhodamine B as standard (ϕ = 0.5, in ethanol) [c]Decomposition temperature at 10% weight loss, determined by TGA. [d]Determined from the onset wavelength of the UV-vis absorption in cyclohexane. [e]Calculated from theoretical study in vacuum.

View Article Online
DOI: 10.1039/C4DT00983E

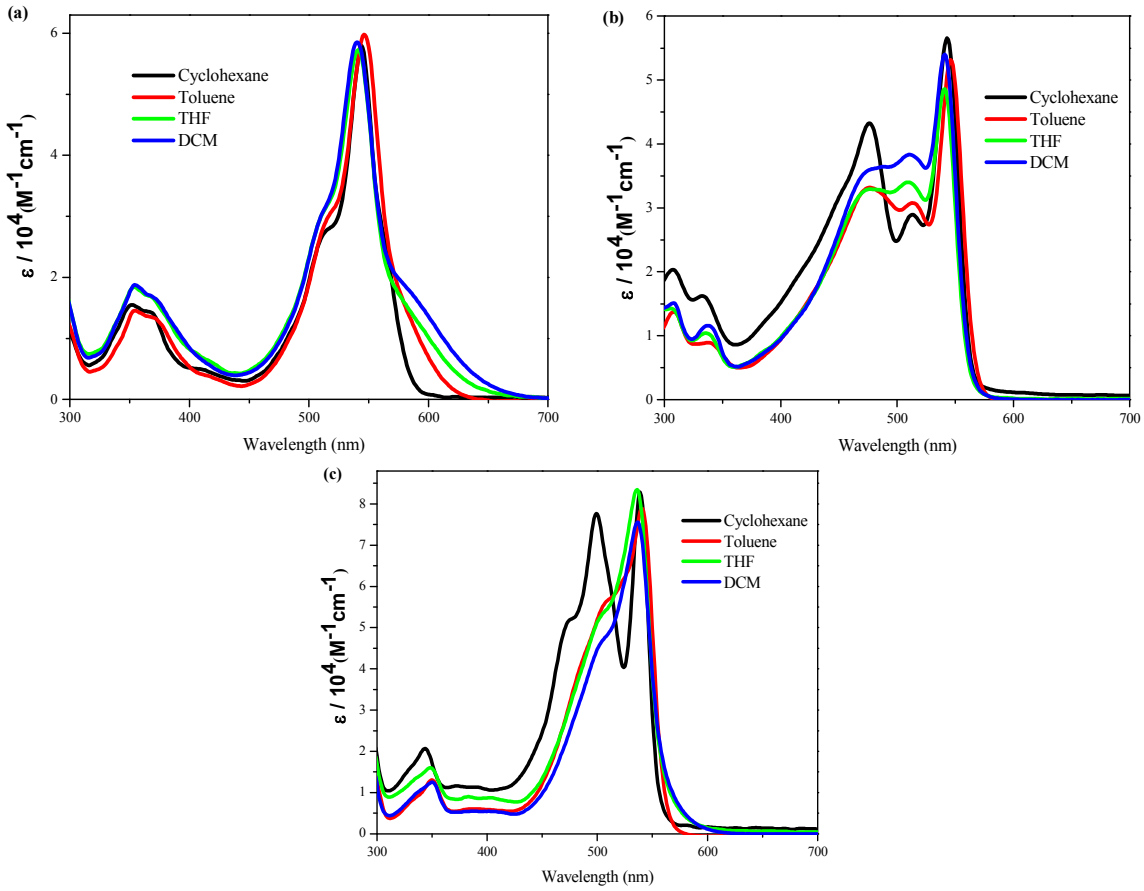

Fig. 3 Absorption spectra of the BODIPYs **2a** (a), **2b** (b), and **2c** (c) in different solvents.

In order to study the effect of solvent variation on the electronic absorption behavior of the BODIPYs **2a-2c**, TD-DFT calculations were performed in dichloromethane and cyclohexane solvents using IEFPCM model. The computed vertical transitions, their oscillator strengths and the configurations are shown in Table 2. The molecular orbitals involved in the transitions are displayed in Fig. S6. The contributions from different orbitals were found to be largely influenced by the polarity of the solvents. The TD-DFT studies exhibit two major transitions for BODIPYs **2a** and **2c**, whereas three major transitions for **2b**. TD-DFT calculations of the BODIPY **2a** in cyclohexane reveal that the main absorption band at 451 nm and weak absorption band at 407 nm are mainly from HOMO-4 and HOMO-2 to the LUMO orbital. The BODIPY **2b**

View Article Online
DOI: 10.1039/C4DT00983E

shows main transition at 480 nm from HOMO-3 and HOMO-2 to the LUMO orbital and two weak bands at 458 and 409 nm from HOMO-3 and HOMO-1 to the LUMO orbital. The BODIPY **2c** shows the main transition at 445 nm and weak transition at 403 nm from HOMO-3 and HOMO-1 to the LUMO orbital.

Table 2. Computed vertical transitions, their oscillator strengths and configurations of BODIPYs **2a-2c**.

Compound	DCM			cyclohexane		
	λ_{max}[nm]	f^a	Configuration	λ_{max}[nm]	f^a	Configuration
2a	472.54	0.5174	HOMO-4 -LUMO(0.19082) HOMO-2 -LUMO(0.68435)	450.65	0.2777	HOMO-4 -LUMO(0.30622) HOMO-3 -LUMO(0.24261) HOMO-2 -LUMO(0.58965)
	413.45	0.1205	HOMO-4 -LUMO(0.67993) HOMO-2 -LUMO(-0.19424)	407.40	0.2000	HOMO-4 -LUMO(0.61773) HOMO-2 -LUMO(0.34555)
2b	517.22	1.1228	HOMO-1-LUMO(0.70434)	479.85	0.9528	HOMO-2 – LUMO(0.70526)
	480.46	0.4795	HOMO-3 - LUMO(-0.15527) HOMO-2 - LUMO(0.69229)	457.72	0.3378	HOMO-3 - LUMO(0.25489) HOMO-1 - LUMO(0.66410)
	413.07	0.0870	HOMO-3- LUMO(0.68861) HOMO-2- LUMO(0.15815)	409.39	0.1138	HOMO-3 -LUMO(0.65791) HOMO-1 -LUMO(-0.25915)
2c	468.27	0.5376	HOMO-4 - LUMO(-0.17930) HOMO-1 - LUMO(-0.68721)	445.38	0.3512	HOMO-3 - LUMO(-0.32036) HOMO-1 - LUMO(-0.63474)
	408.49	0.1144	HOMO-4 - LUMO(-0.68302) HOMO-1 - LUMO(0.18244)	403.19	0.1916	HOMO-3 - LUMO(-0.62915) HOMO-1 - LUMO(0.32614)

[a] Oscillator strength

The fluorescence spectra of BODIPYs **2a-2c** in different solvents are shown in the Fig. 4 and data are summarized in Table 1. The fluorescence spectra of **2a-2c** in nonpolar solvent exhibits characteristic emission of BODIPYs such as narrow bandwidth, small stokes shift and high quantum yield. The increase in solvent polarity leads to red shift in the fluorescence with decrease in fluorescence quantum yield and generates a new broad emission band at longer

View Article Online
DOI: 10.1039/C4DT00983E

wavelength region. The emission band in nonpolar solvent was assigned as locally excited (LE) emission band while the newly generated longer wavelength emission band in polar solvent was assigned as charge transfer (CT) emission band.[9,11]

The literature reveals that the contribution of emission from CT state in BODIPYs is directly proportional to the strength of donor-acceptor interaction.[9] The emission from charge transfer state and quenching of fluorescence could be an effective tool to compare the strength of D-A interactions in the BODIPYs.[4,9] The BODIPYs **2a-2c** show different emission patterns with increasing the solvent polarity from cyclohexane to toluene and tetrahydrofuran. The emission is dominated from CT state with decrease in the quantum yield by increasing the polarity of solvent. The BODIPYs **2a-2c** emit from the LE state in non-polar solvent (cyclohexane) with high quantum yields. In toluene the BODIPYs **2b** and **2c** show emission from LE state, whereas **2a** shows emission from CT state. In THF **2b** show dual emission LE and CT state whereas **2a** and **2c** show emission from CT state. The BODIPY **2a** show considerable red shift in the emission with decrease in quantum yield from cyclohexane to toluene and THF, indicating that some additional factors are also involved. The two *ter*-butyl groups on the carbazole unit decreases the quantum yield due to rotational and vibrational relaxations and may have important role in more donor-acceptor character.[12,13] The polar dichloromethane solvent stabilizes the charge transfer state and makes the BODIPYs **2a-2c** non-emissive. The emission properties of BODIPYs **2a-2c** in different solvents suggest the trend in strength of D-A interaction as **2a** > **2c** > **2b.** The high sensitivity of the BODIPYs **2a-2c** towards solvent polarity make them potential candidate for application as fluorescent probes for biological species and solvent polarity detection.[10]

View Article Online
DOI: 10.1039/C4DT00983E

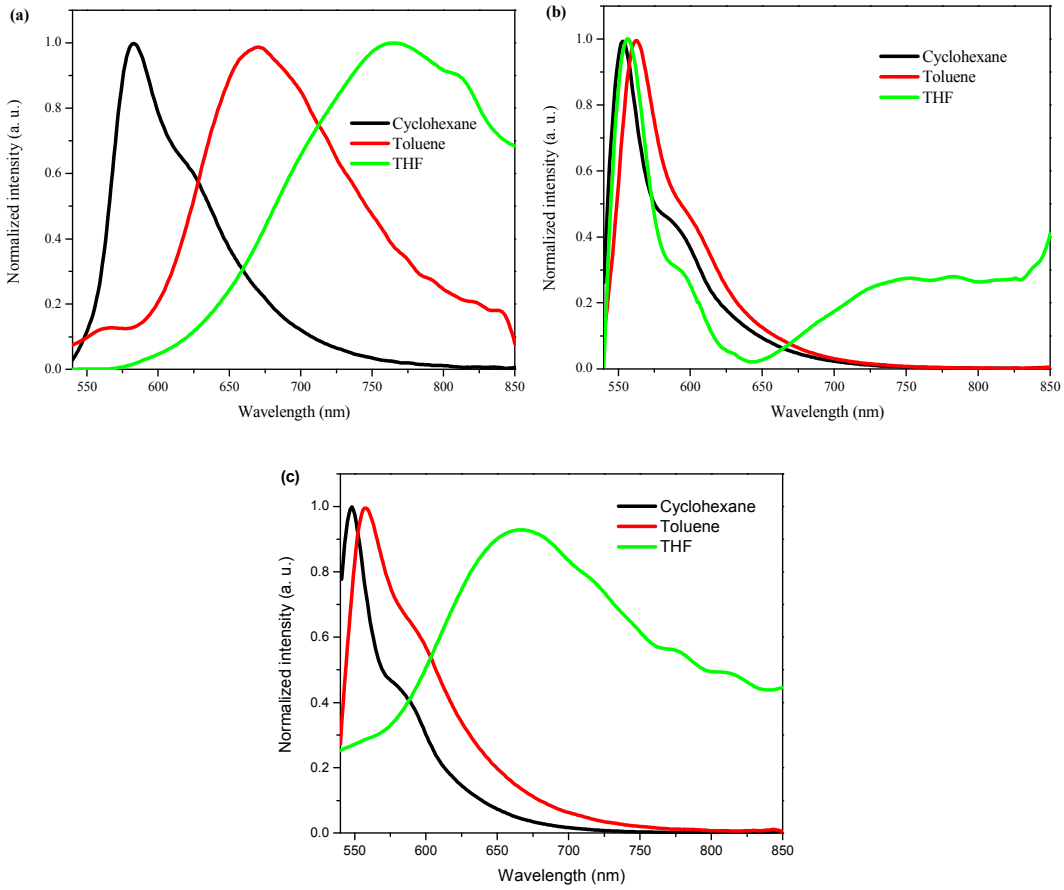

Fig. 4 Normalized fluorescence spectra at the wavelength of maximum intensity of **2a** (a), **2b** (b), and **2c** (c) in cyclohexane, toluene and THF solvents.

View Article Online
DOI: 10.1039/C4DT00983E

Electrochemical properties

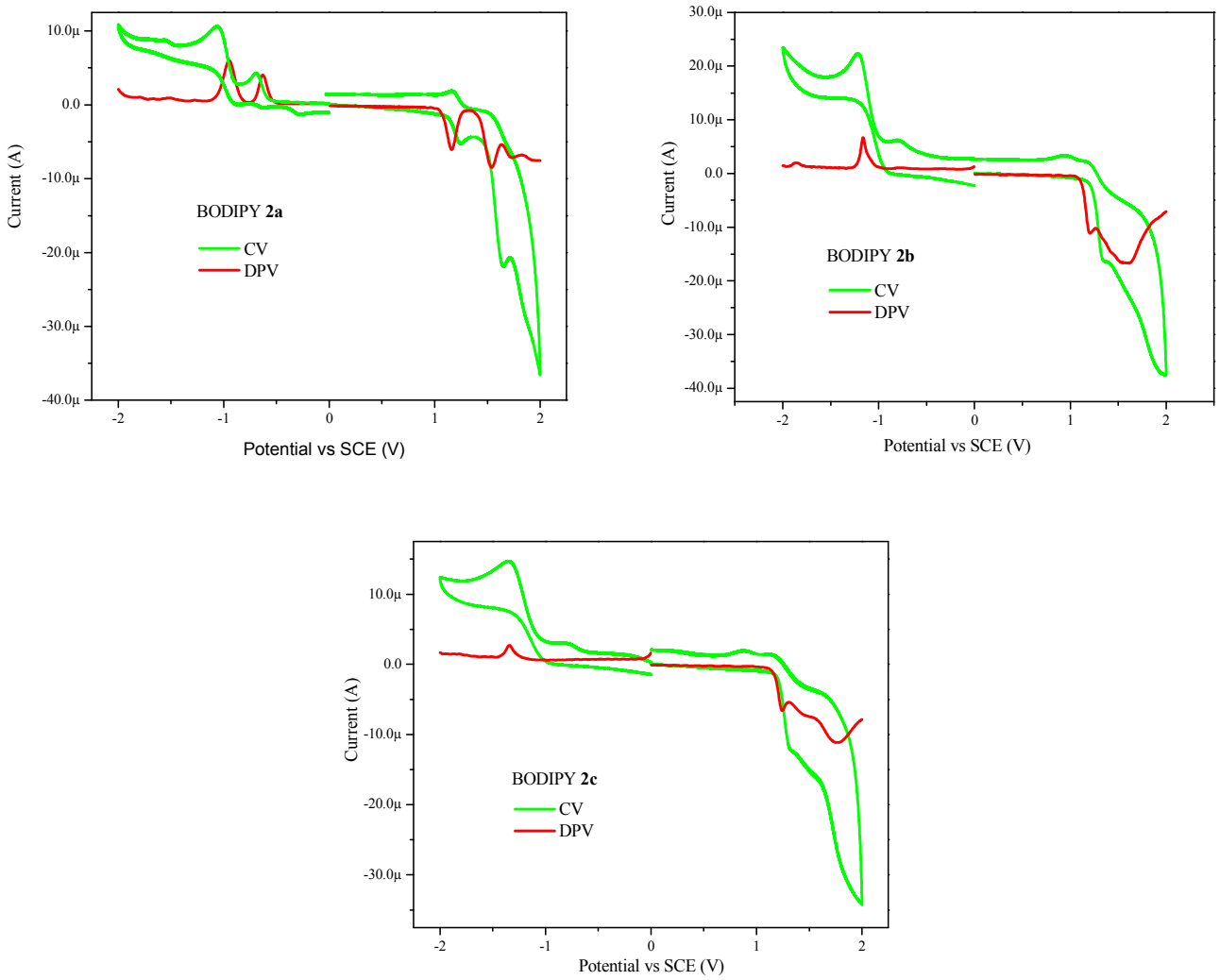

Fig. 5 The CV and DPV plots of the BODIPYs **2a-2c**.

The electrochemical properties of the BODIPYs **2a-2c** were investigated by the cyclic voltammetric and differential pulse voltammetric (CV and DPV) techniques. The CV and DPV results are shown in Fig. 5 and the corresponding data are summarized in Table 3. The electrochemical study reveals that the redox peaks are irreversible in nature. The BODIPY **2a** show two oxidation and two reduction waves corresponding to the formation of dication and

View Article Online
DOI: 10.1039/C4DT00983E

dianion radicals respectively, whereas BODIPYs **2b** and **2c** show two oxidation and one reduction waves corresponding to the formation of dication and anion radicals respectively. The BODIPY **2a** shows the easiest oxidation indicating the pronounced delocalization of the electron density of the donor carbazole moiety in the acceptor BODIPY. The trend in the first oxidation potential follows the order as **2b> 2c** > **2a.** This trend supports the strength of donor-acceptor interaction observed from the photophysical studies.

Table 3. Electrochemical properties of the BODIPYs **2a-2c**.[a]

BODIPY	E^2_{oxid}[b]	E^1_{oxid}[b]	E^1_{red}[b]	E^2_{red}[b]
2a	1.54	1.16	-0.63	-0.95
2b	1.77(broad)	1.24	-1.34	-
2c	1.58(broad)	1.21	-1.16	-

[a] electrochemical analysis was performed in 0.1 M solution of Bu_4NPF_6 in DCM at 100 mV s^{-1} scan rate, versus SCE. [b]irreversible wave.

Theoretical calculations

In order to understand the geometry and the electronic structure of the BODIPYs **2a-2c** density functional theory (DFT) calculations were carried out using the Gaussian09W program.[14] The geometry optimization was carried out without any symmetry constraint in the gas phase. The density functional theory (DFT) calculation was performed at the B3LYP/6-31G (d) level of theory.[14] The TD-DFT calculations were performed at the B3LYP/6-31 G(d) level .[15]

The geometry optimization show good correlations with the experimental data obtained from single crystal structures. The Fig. 6 depicts the frontier molecular orbitals (FMO) of the BODIPYs **2a-2c**. In BODIPY **2a**, HOMO is localized on the electron donating carbazole unit

View Article Online
DOI: 10.1039/C4DT00983E

and LUMO on the electron withdrawing BODIPY unit, which reflects strong donor-acceptor interaction. In BODIPYs **2b** and **2c** HOMO is localized on the BODIPY unit and LUMO on the BODIPY and carbazole unit, which reveals weak donor-acceptor interaction than **2a**. The theoretical band gap values are summarized in Table 1, which shows the trend as **2a** < **2b** < **2c**.

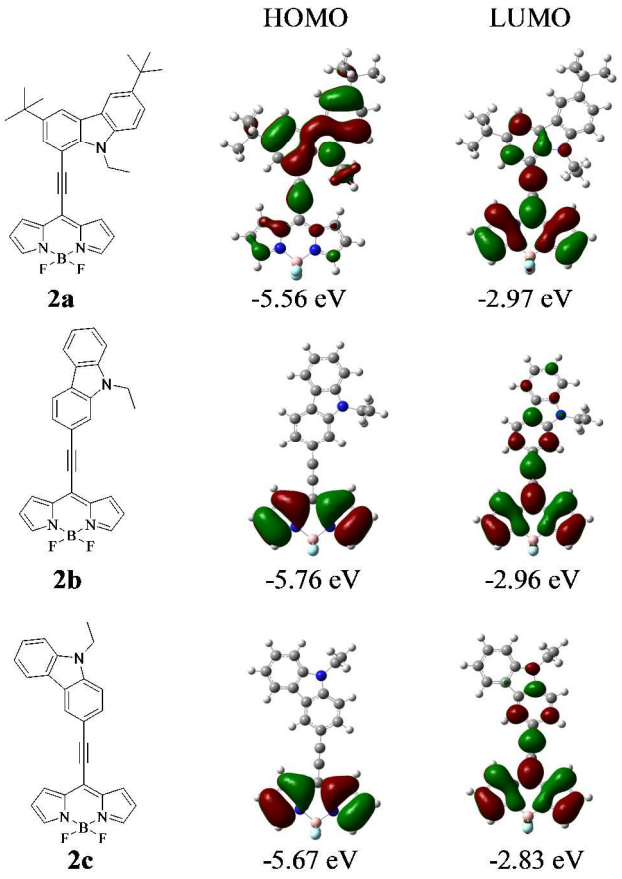

Fig. 6 Frontier molecular orbitals of BODIPYs **2a-2c** at the B3LYP/6-31G(d) level.

View Article Online
DOI: 10.1039/C4DT00983E

Single crystal X-ray analysis

The single crystals of the BODIPYs **2a** and **2b** were obtained by slow diffusion of ethanol in the dichloromethane solution whereas crystal of **2c** was obtained by slow evaporation of hexane:dichloromethane (6:4) solution at room temperature. The BODIPYs **2a**–**2c** crystallizes into orthorhombic *P*na2_1, *P*$2_1$$2_1$$2_1$, and *P*bcn space groups respectively. The crystal structure and data refinement parameters are shown in Table S1 (SI). The front view and side view of the crystal structures are displayed in Fig. 7. The crystal structures of BODIPYs **2a**–**2c** show planar structures. The dihedral angle between carbazole and BODIPY units in BODIPYs **2a**–**2c** are 24.77°, 4.04°, and 8.25° respectively.

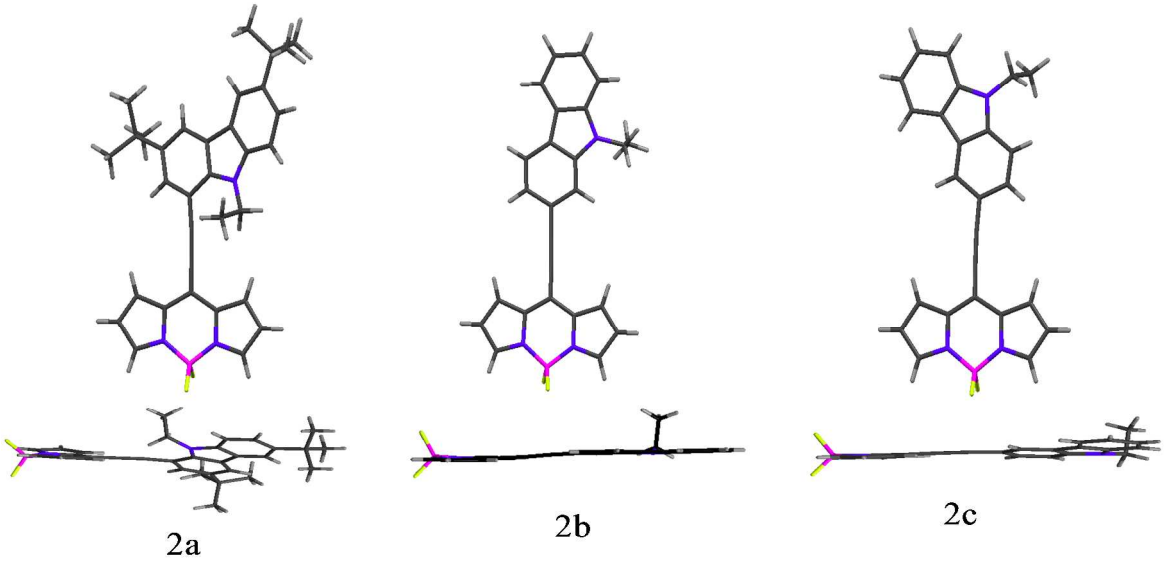

Fig. 7 Crystal structures of the BODIPYs **2a-2c**, (A) front view and (B) side view.

The comparison of the selected bond lengths and bond angles of the single crystal structures and the DFT optimized structures of BODIPYs **2a**–**2c** show slight variation in bond lengths and bond angles (Fig. 8 and Fig. S5). In the BODIPYs **2a**–**2c** the two C-N bonds of carbazole show different bond lengths. The C-N bond near to BODIPY is shorter than the distant C-N bond,

View Article Online
DOI: 10.1039/C4DT00983E

suggesting higher double bond character of the former, due to the delocalization of lone pair electrons of carbazole nitrogen into the electron deficient BODIPY unit.[16]

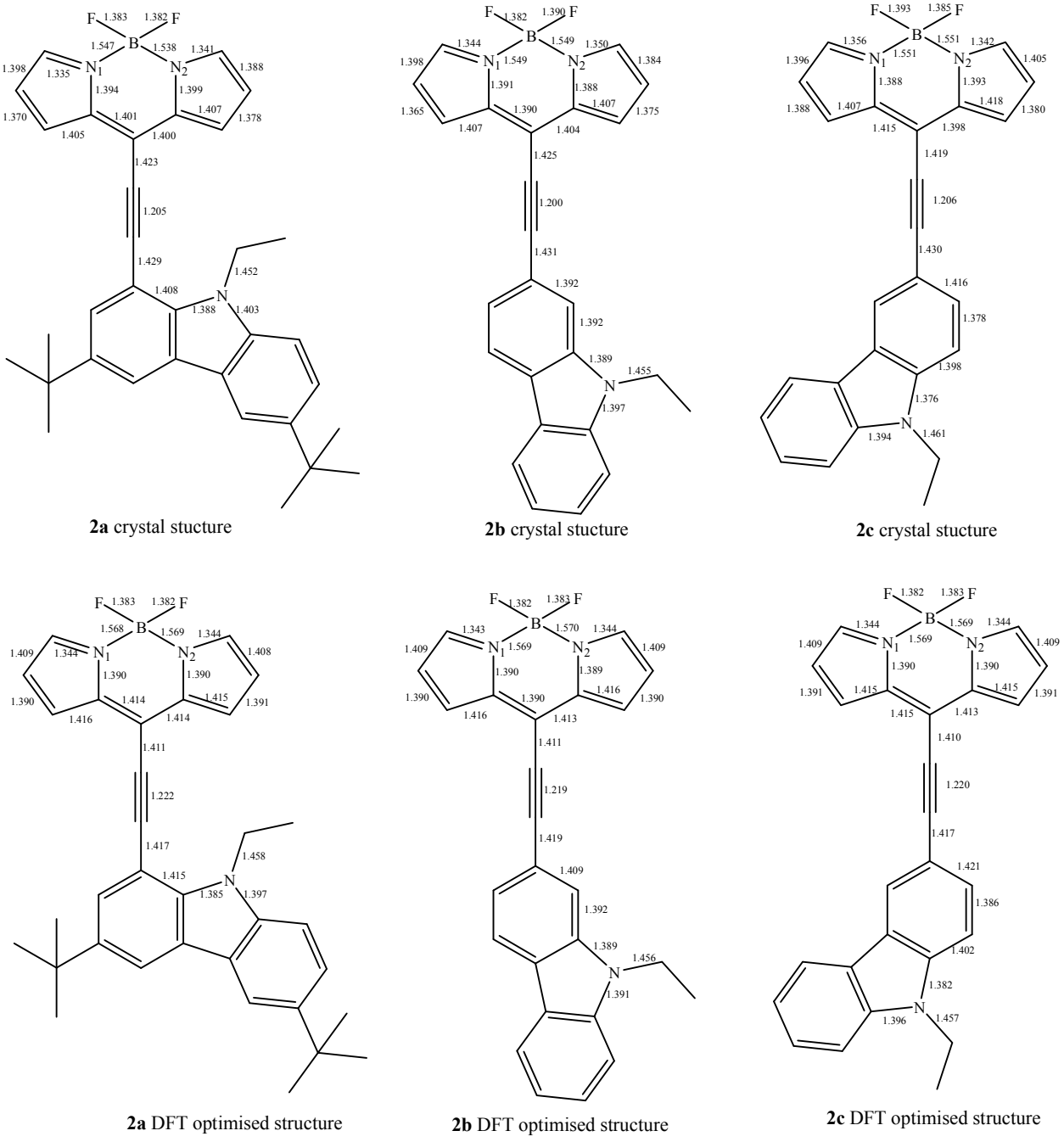

Fig. 8 Comparison of selected bond lengths of the crystal structures and DFT optimized structures of the BODIPYs **2a-2c**.

View Article Online
DOI: 10.1039/C4DT00983E

The crystal structures of the BODIPYs **2a-2c** show interesting supramolecular interactions. The distances of the supramolecular interactions in the crystal packing are shown in Table 3. In the packing diagram of **2a**, the interactions C(8)-H(8)---F(2), C(13)-H(13)---F(2) and C(25A)-H(25A)---F(2) form a trimer like structure which grows along the *c*-axis to form 2D sheet (Fig. S4). The two different sheets connect another via C(15)-H(15)---F(1), C(22)-H(22)---F(1) and C(13)-H(13)---F(2) interactions to form *zig zag* 3D structural arrangement (Fig. 9).

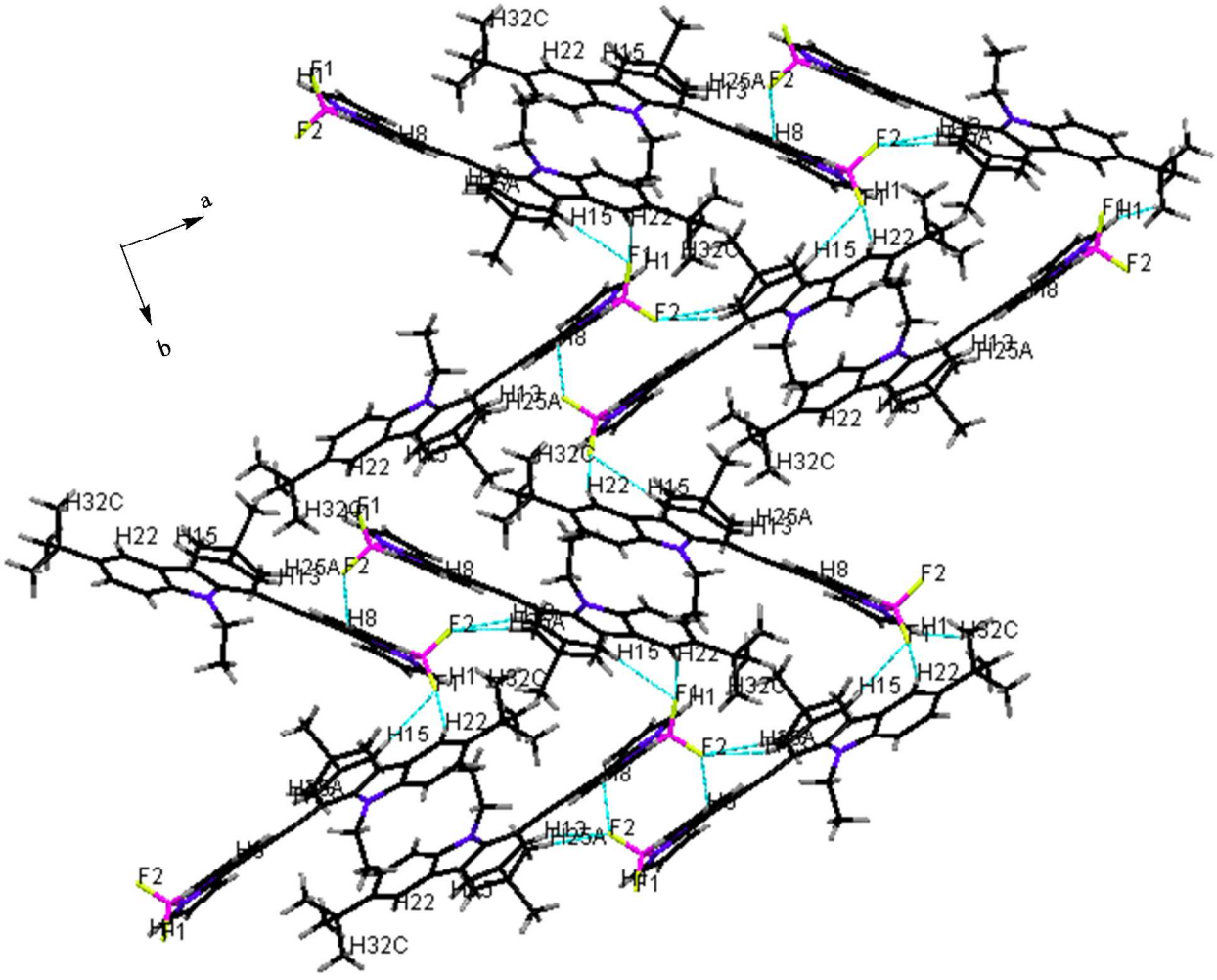

Fig. 9 Packing diagram of the BODIPY **2a.**

View Article Online
DOI: 10.1039/C4DT00983E

In the packing diagram of BODIPY **2b**, the interaction F(1)---H(13)-C(13) and C(2)-H(2)---π (centroid C6, C7, C8, C9, N2) leads to the Z-shaped 2D chain. This 2D chain further transforms into a sheet through interactions C(16)-H(16)---π (centroid C12, C13, C14, C15, C16, C17), C(8)-H(8)---π (centroid C1, C2, C3, C4, N1), π (centroid C1, C2, C3, C4, N1)--- π (centroid C6, C7, C8, C9, N2). This two dimensional chain further extends to complex 3D structural motifs via two mutual C(1)-H(1)---F(2) interactions (Fig. 10).

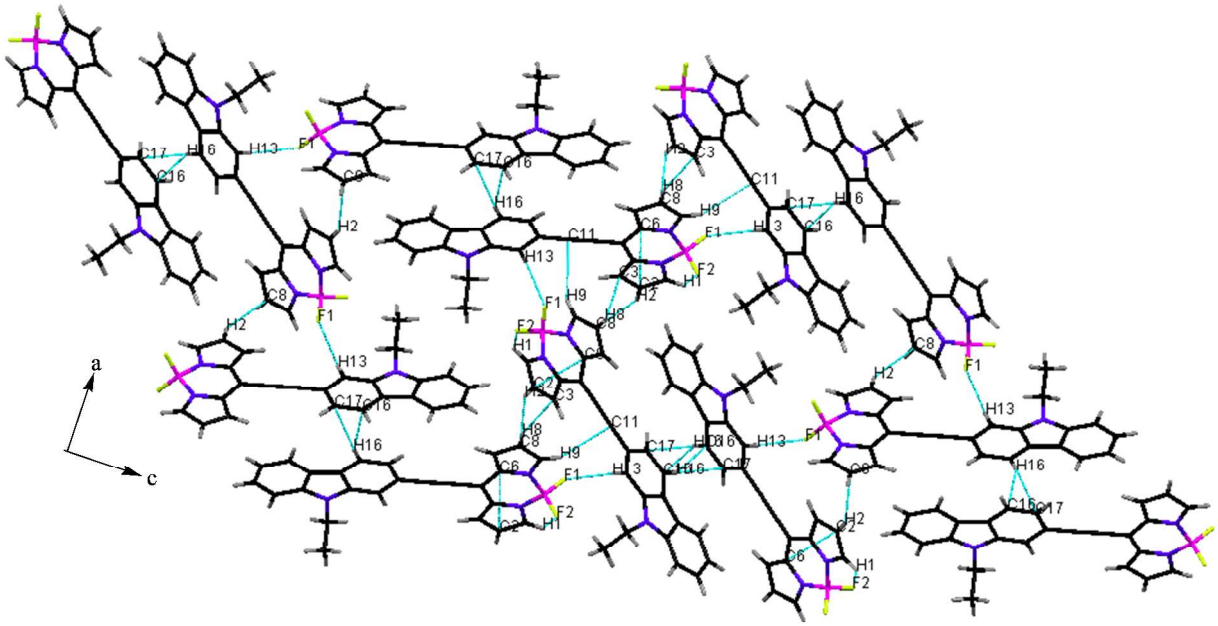

Fig. 10 Packing diagram of the BODIPY **2b.**

In the packing diagram of BODIPY **2c** the interaction C(9)-H(9) ---F(1) forms a herringbone like structure, in which the BODIPY core is connected to each other in head to heat fashion along *c*-axis (Fig. 11a). This sheet further grow in above direction via C(21)-H(21)---F(2), C(25C)-H(25C)--- F(2), C(1)-H(1)---π (centroid C18, C19, C20, C21, C22, C23) interactions and

View Article Online
DOI: 10.1039/C4DT00983E

in below direction via C(24B)-H(24B)---F(1), and C(24A)-H(24A)---π (centroid C6, C7, C8, C9, N2) interactions to form complex 3D structural arrangement (Fig. 11b).

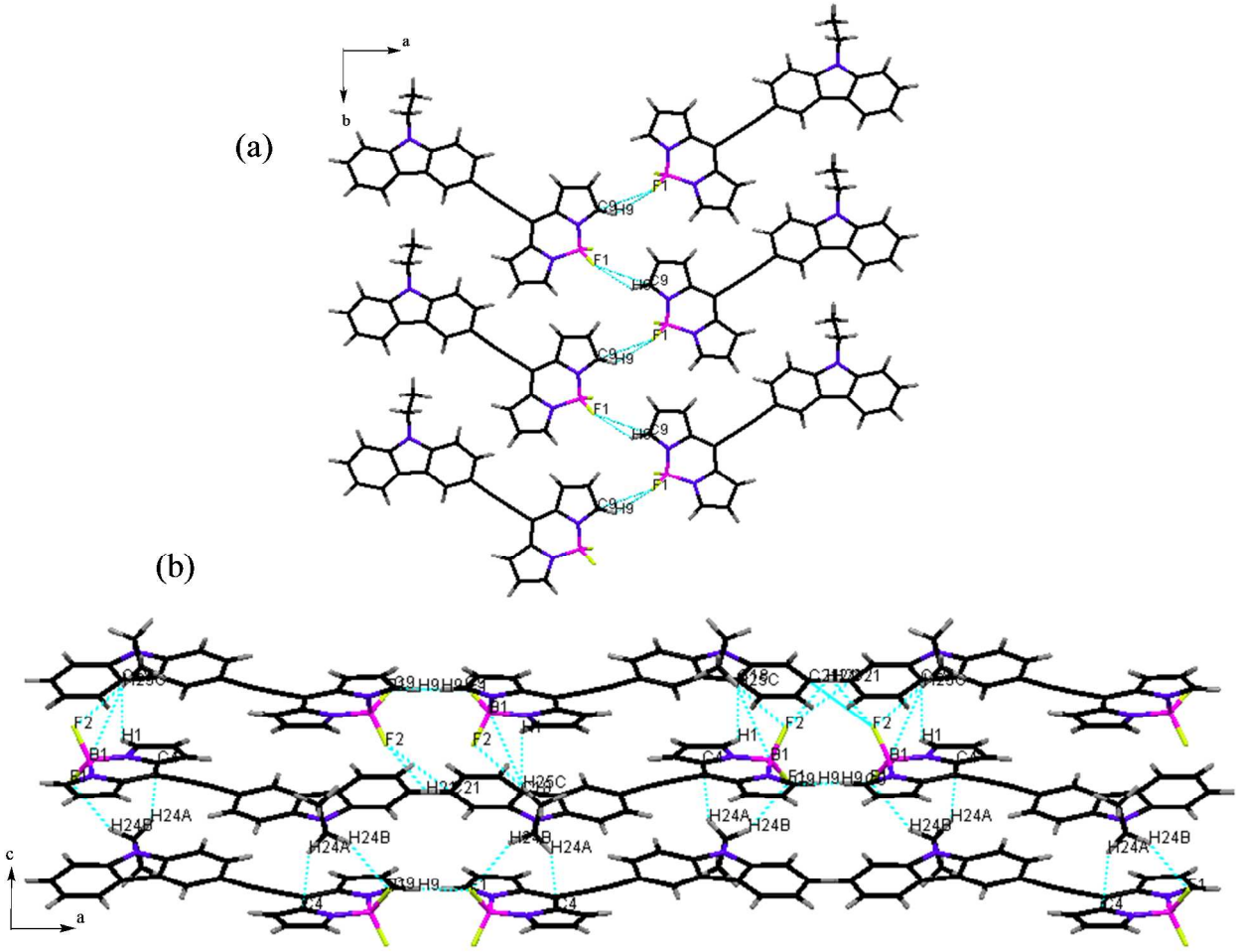

Fig. 11 Packing diagram of the BODIPY **2c** (a) view along *c*-axis (b) view along *b*-axis.

View Article Online
DOI: 10.1039/C4DT00983E

Table 3. Selected bond length of intermolecular interactions in the crystal structure of BODIPYs **2a-2c.**

Interaction	Distance (Å)
2a	
C(15)-H(15)---F(1)	2.628
C(22)-H(22)---F(1)	2.626
C(13)-H(13)---F(2)	2.478
C(25A)-H(25A)---F(2)	2.574
C(8)-H(8)---F(2)	2.552
2b	
C(16)-H(16)---π (centroid C12, C13, C14, C15, C16, C17)	2.806
C(8)-H(8)---π (centroid C1, C2, C3, C4, N1)	3.216
C(9)-H(9)---π (acetylene)	2.928
π (centroid C1, C2, C3, C4, N1) --- π (centroid C6, C7, C8, C9, N2)	3.434
C(2)-H(2)---π (centroid C6, C7, C8, C9, N2)	3.175
C(13)-H(13)--- F(1)	2.489
C(1)-H(1)---F(2)	2.602
2c	
C(9)-H(9)---F(1)	2.426
C(24B)-H(24B)---F(1)	2.514
C(24A)-H(24A)---π (centroid C6, C7, C8, C9, N2)	2.655
C(21)-H(21)---F(2)	2.532
C(25C)-H(25C)--- F(2)	2.545
C(1)-H(1)---π (centroid C18, C19, C20, C21, C22, C23)	3.014

Conclusion

In summary donor-acceptor carbazole-BODIPY conjugates **2a-2c** were synthesized by the Pd-catalysed Sonogashira cross-coupling reaction. The electronic absorption and fluorescence properties show intramolecular charge transfer from carbazole to BODIPY. The photophysical properties of BODIPYs **2a-2c** in different solvents suggest that the *meso*-ethynylBODIPY can be used as effective tool to measure small differences in donor strength of different carbazoles. The donor-acceptor interaction in BODIPYs **2a-2c** follows the order **2a** > **2c** > **2b**. The presence of alkyl groups and steric hindrance in BODIPY **2a** decreases the thermal stability. Our results provide important method for screening the donor strength of different donors which will help in design of strong D-A materials.

View Article Online
DOI: 10.1039/C4DT00983E

Experimental Section

General methods.

Chemicals were used as received unless otherwise indicated. All oxygen or moisture sensitive reactions were performed under nitrogen/argon atmosphere. ^{1}H NMR (400 MHz), and ^{13}C NMR (100MHz) spectra were recorded on the Bruker Avance (III) 400 MHz instrument by using $CDCl_3$. ^{1}H NMR chemical shifts are reported in parts per million (ppm) relative to the solvent residual peak ($CDCl_3$, 7.26 ppm). Multiplicities are given as: s (singlet), d (doublet), t (triplet), q (quartet), dd (doublet of doublets), dt (doublet of triplets), m (multiplet), and the coupling constants, *J*, are given in Hz. ^{13}C NMR chemical shifts are reported relative to the solvent residual peak ($CDCl_3$, 77.36 ppm. Thermogravimetric analyses were performed on the Metler Toledo Thermal Analysis system. UV-visible absorption spectra were recorded on a Carry-100 Bio UV-visible Spectrophotometer. Cyclic voltamograms (CVs) were recorded on a CHI620D electrochemical analyzer using Glassy carbon as working electrode, Pt wire as the counter electrode, and Saturated Calomel Electrode (SCE) as the reference electrode. The scan rate was 100 mVs^{-1}. A solution of tetrabutylammonium hexafluorophosphate ($TBAPF_6$) in CH_2Cl_2 (0.1 M) was employed as the supporting electrolyte. HRMS was recorded on Brucker-Daltonics, micrOTOF-Q II mass spectrometer. The density functional theory (DFT) calculation were carried out at the B3LYP/6-31G(d) level for B, F, C, N, H in the Gaussian 09 program.

Synthesis and Characterization of BODIPYs 2a-2c:

A generalized procedure for the Sonogashira cross-coupling reaction.

8-Chloro BODIPY **1** (190 mg, 0.845 mmol) and the corresponding ethynyl-carbazole (0.845 mmol) were dissolved in DCM–triethylamine (10 : 1, v/v; 10 ml), and the mixture was cooled to

View Article Online
DOI: 10.1039/C4DT00983E

0 °C using an ice bath. The reaction mixture was purged with argon, and $Pd(PPh_3)_2Cl_2$ (29.6 mg, 5 mol%), and CuI (16 mg, 10 mol%) were added, followed by stirring at 0-5 °C for 1 h. Upon the completion of the reaction, the mixture was evaporated to dryness, and the crude product was dissolved in CH_2Cl_2, chromatographed on silica (5:5; hexanes:dichloromethane), and recrystallized from a DCM:Ethanol (8:2) mixture to gave **2a-2c** (yield 55–70%) as crystalline solids.

2a

Blue solid. Yield: 69%, Mp: above 250 °C. ^{1}H NMR (400 MHz, $CDCl_3$, 25 °C, ppm): δ 8.27 (d, 1H, *J*=4 Hz), 8.12 (d, 1H, *J*=4 Hz), 7.86 (s, 2H), 7.75 (d, 1H, *J*=2 Hz), 7.61 (dd, 1H, *J*=1.6, 8 Hz), 7.44 (d, 2H, *J*=4 Hz), 7.39 (d, 1H, *J*=12 Hz), 6.6 (d, 2H, *J*=4 Hz), 4.89 (q, 2H, *J*=8 Hz), 1.50-1.55 (m, 12H), 1.48 (s, 9H) ppm, 0.00 ppm; ^{13}C NMR (100 MHz, $CDCl_3$, 25 °C, ppm): δ 143.1,143.0, 141.9, 138.9, 137.6, 136.4, 130.3, 128.3, 127.9, 124.9, 124.6, 122.2, 121.1, 118.3, 118.2, 116.4, 108.4, 106.9, 101.2, 88.1, 38.6, 34.7, 34.6, 32.0, 31.8, 15.0; ^{11}B NMR ($CDCl_3$, 96.3 MHz, ppm) 0.3 (t, $J_{B\text{-}F}$ = 19.3 Hz); HRMS (ESI-TOF) m/z: calcd. for $C_{33}H_{34}BF_2N_3 + H^+$ = 522.2892, found 522.2896.

2b

Red solid, Yield: 58%, Mp: above 250 °C. ^{1}H NMR (400 MHz, $CDCl_3$, 25 °C, ppm): δ 8.13-8.17 (m, 2H), 7.85 (s, 2H), 7.71 (s, 1H), 7.46-7.58 (m, 5H), 7.28-7.32 (m, 1H), 6.58 (d, 2H, *J*=4 Hz), 4.44 (q, 2H, *J*=8 Hz), 1.50 (t, 3H, *J*=8 Hz) ppm; ^{13}C NMR (100 MHz, $CDCl_3$, 25 °C, ppm): δ 143.2, 141.2, 139.3, 136.5, 128.9, 127.4, 125.4, 123.6, 122.3, 121.2, 120.8, 119.7, 118.2, 117.1, 113.0, 108.9, 108.7, 84.5, 37.8, 13.9, 0.00 ppm; ^{11}B NMR ($CDCl_3$, 96.3 MHz, , ppm) 0.2 (t, $J_{B\text{-}F}$ = 19.3 Hz); HRMS (ESI-TOF) m/z: calcd. for $C_{25}H_{18}BF_2N_3 + Na^+$ = 432.1458, found 432.1451.

View Article Online
DOI: 10.1039/C4DT00983E

2c

Red solid Yield: 70%, Mp: 222-226 °C. ^{1}H NMR (400 MHz, $CDCl_3$, 25 °C, ppm): δ 8.43 (dd, 1H, *J*=2, 0.8 Hz), 8.14-8.16 (m, 1H), 7.82 (s, 2H), 7.76 (dd, 1H, *J*=8.8, 1.2 Hz), 7.54-7.58 (m, 1H), 7.45-7.49 (m, 4H), 7.32-7.36 (m, 1H), 6.57 (d, 2H, *J*=4 Hz), 4.42 (q, 2H, *J*=8 Hz), 1.49 (t, 3H, *J*=8 Hz) ppm; ^{13}C NMR (100 MHz, $CDCl_3$, 25 °C, ppm): δ 142.4, 141.3, 140.5, 136.3, 130.6, 126.4, 126.9, 126.2, 123.5, 122.3, 120.8, 120.3, 117.9, 110.6, 109.12, 109.06, 84.8, 37.9, 13.8. ^{11}B NMR ($CDCl_3$, 96.3 MHz, , ppm) 0.3 (t, $J_{B\text{-}F}$ = 19.3 Hz); HRMS (ESI-TOF) m/z: calcd. for $C_{25}H_{18}BF_2N_3 + Na^+$ = 432.1458, found 432.1452.

Supporting Information

General experimental methods, and copies of ^{1}H, ^{13}C, ^{11}B, ^{19}F NMR, and HRMS spectra of all new compounds, Crystallographic Information Files (CIFs) for **2a-2c** with CCDC numbers 994993, 994994 and 994991 respectively, and DFT calculation data.

Acknowledgment

We thank CSIR, and DST, New Delhi for financial support. TJ and BD thanks, UGC and CSIR New Delhi for their fellowship. We are thankful to Sophisticated Instrumentation Centre (SIC), IIT Indore.

REFERENCES

1 (a) O. A. Bozdemir, R. Guliyev, O. Buyukcakir, S. Selcuk, S. Kolemen, G. Gulseren, T. Nalbantoglu, H. Boyaci and E. U. Akkaya, *J. Am. Chem. Soc.*, 2010, **132**, 8029; (b) S. J. Lord, N. R. Conley, H. L. D. Lee, R. Samuel, N. Liu, R. J. Twieg and W. E. Moerner, *J. Am. Chem. Soc.,* 2008, **130**, 9204-9205; (c) S. R. Marder, B. Kippelen, A. K. Y. Jen and N. Peyghammbarian,

View Article Online
DOI: 10.1039/C4DT00983E

Nature, 1997, **388**, 845-851; (d) S. M. LeCours, H. W. Guan, S. G. DiMagno, C. H. Wang and M. J. Therien, *J. Am. Chem. Soc.,* 1996, **118**, 1497-1503; (e) X. Yin, Y. Li, Y. Li, Y. Zhu, X. Tang, H. Zheng and D. Zhu, *Tetrahedron,* 2009, **65**, 8373–8377; (f) V. N. Nemykin, E. A. Makarova, J. O. Grosland, R. G. Hadt and A. Y. Koposov, *Inorg. Chem.,* 2007, **46**, 9591−9601; (g) X. Yin, Y. Li, Y. Zhu, X. Jing, Y. Li and D. Zhu, *Dalton Trans*., 2010, **39**, 9929-9935; (h) G. Ulrich, R. Ziessel and A. Harriman, *Angew. Chem. Int. Ed.,* 2008, **47**, 1184-1201; (i) M. E. El-Khouly, S. Fukuzumi and F. D'Souza, *ChemPhysChem.,* 2014, **15**, 30-47; (j) A. Loudet and K. Burgess, *Chem. Rev.,* 2007**, 107**, 4891–4932.

2 (a) N. Boens, V. Leen and W. Dehaen, *Chem. Soc. Rev.,* 2012, **41**, 1130–1172; (b) A. Coskun, M. Yilmaz and E. U. Akkaya, *Org. Lett*., 2007, **9**, 607–609; (c) J. Han, A. Loudet, R. Barhoumi, R. C. Burghardt and K. Burgess, *J. Am. Chem. Soc*., 2009, **131**, 1642–1643; (d) T. Yogo, Y. Urano, Y. Ishitsuka, F. Maniwa and T. Nagano, *J. Am. Chem. Soc.*, 2005, **127**, 12162–12163; (e) D. Kumaresan, R. P. Thummel, T. Bura, G. Ulrich and R. Ziessel, *Chem. Eur. J*., 2009, **15**, 6335–6339; (f) S. Kolemen, Y. Cakmak, S. Erten-Ela, Y. Altay, J. Brendel, M. Thelakkat and E. U. Akkaya, *Org. Lett.*, 2010, **12**, 3812–3815; (g) M. T. Whited, P. I. Djurovich, S. T. Roberts, A. C. Durrell, C. W. Schlenker, S. E. Bradforth and M. E. Thompson, *J. Am. Chem. Soc.*, 2011, **133**, 88–96; (h) J. Lehl, J.-F. Nierengarten, A. Harriman, T. Bura and R. Ziessel, *J. Am. Chem. Soc.*, 2012, **134**, 988–998; (i) Q. Zheng, G. Xu and P. Prasad, *Chem.–Eur. J*., 2008, **14**, 5812–5819; (j) P. Didier, G. Ulrich, Y. Mely and R. Ziessel, *Org. Biomol. Chem.*, 2009, **7**, 3639–3642; (k) P. A. Bouit, K. Kamada, P. Feneyrou, G. Berginc, L. Toupet, O. Maury and C. Andraud, *Adv. Mater.*, 2009, **21**, 1151–1154.

3 (a) R. Misra, B. Dhokale, T. Jadhav, S. M. Mobin, *Dalton Trans.,* 2013, **42**, 13658. (b) P. Gautam, B. Dhokale, S. M. Mobin, R. Misra, *RSC Adv.,* 2012, **2**, 12105-12107. (c) R. Misra, B.

View Article Online
DOI: 10.1039/C4DT00983E

Dhokale, T. Jadhav, S. M. Mobin, *Organometallics,* 2014, **33**, 1867–1877. (d) B. Dhokale, P. Gautam, S. M. Mobin, R. Misra, R. *Dalton Trans.,* 2013, **42**, 1512–1518. (e) B. Dhokale, T. Jadhav, S. M. Mobin and R. Misra, *Chem. Commun.*, 2014, DOI: 10.1039/C4CC03857F.

4 R. Misra, B. Dhokale, T. Jadhav, S. M. Mobin, *Dalton Trans.,* 2014, **43**, 4854-4861.

5 (a) J. V. Grazulevicius, P. Strohriegl, J. Pielichowski, K. Pielichowski, *Prog. Polym. Sci.,* 2003, **28**, 1297. (b) J. F. Morin, M. Leclerc, D. Adès, A. Siove, *Macromol. Rapid Commun.,* 2005, **26**, 761. (c) N. Blouin, M. Leclerc, *Acc. Chem. Res.,* 2008, **41**, 1110. (d) S. Sujeewa, X. C. Palayangoda, R. M. Adhikari, D. C. Neckers, *Org. Lett.,* 2008, **10**, 4. (d) J. Li, A. C. Grimsdale, *Chem. Soc. Rev.,* 2010, **39**, 2399.

6 (a) S. I. Kato, S. Shimizu, H. Taguchi, A. Kobayashi, S. Tobita, Y. Nakamura, *J. Org. Chem.,* 2012, **77**, 3222. (b) S. I. Kato, H. Noguchi, A. Kobayashi, T. Yoshihara, S. Tobita, Y. Nakamura, *J. Org. Chem.,* 2012, **77**, 9120.

7 V. Leen, P. Yuan, L. Wang, N. Boens, W. Dehaen, *Org. lett*., 2012, **14**, 6150.

8 (a) M. Tavasli, S. Bettington, M. R. Bryce, A. S. Batsanov, A. P. Monkman, *Synthesis,* 2005, **10**, 1619. (b) J. I. G. Cadogan, M. Cameron-Wood, *J. Chem. Soc.,* 1962, 361. (c) J. F. Morin, M. Leclerc, *Macromolecules,* 2001, **34**, 4680. (d) Y. Liu, M. Nishiura, Y. Wang, Z. Hou, *J. Am. Chem. Soc.,* 2006, **128**, 5592−5593.

9 W. Qin, M. Baruah, M. Van der Auweraer, F. C. De Schryver, N. Boens, *J. Phys. Chem. A,* 2005, **109**, 7371−7384.

10 E. Lager, J. Liu, A. Aguilar-Aguilar, B. Z. Tang and E. Pena-Cabrera, *J. Org. Chem.,* 2009, **74**, 2053.

11 K. Rurack, M. Kollmansberger, U. Resch-Genger, J. Daub, *J. Am. Chem. Soc.,* 2000, **122**, 968.

View Article Online
DOI: 10.1039/C4DT00983E

12 Y. Gong, Y. Tan, J. Liu, P. Lu, C. Feng, W. Yuan, Y. Lu, J. sun, G. He and Y. Zhang, *Chem. Commun.*, 2013, **49**, 4009.

13 Z. R. Grabowski, K. Rotkiewics and W. Rettig, *Chem. Rev.* 2003, **103**, 3899.

14 (a) M. J. Frisch, G. W. Trucks, H. B. Schlegel, G. E. Scuseria, M. A. Robb, J. R. Cheeseman, G. Scalmani, V. Barone, B. Mennucci, G. A. Petersson, H. Nakatsuji, M. Caricato, X. Li, H. P. Hratchian, A. F. Izmaylov, J. Bloino, G. Zheng, J. L. Sonnenberg, M. Hada, M. Ehara, K. Toyota, R. Fukuda, J. Hasegawa, M. Ishida, T. Nakajima, Y. Honda, O. Kitao, H. Nakai, T. Vreven, J. A. Jr. Montgomery, J. E. Peralta, F. Ogliaro, M. Bearpark, J. J. Heyd, E. Brothers, K. N. Kudin, V. N. Staroverov, R. Kobayashi, J. Normand, K. Raghavachari, A. Rendell, J. C. Burant, S. S. Iyengar, J. Tomasi, M. Cossi, N. Rega, N. J. Millam, M. Klene, J. E. Knox, J. B. Cross, V. Bakken, C. Adamo, J. Jaramillo, R. Gomperts, R. E. Stratmann, O. Yazyev, A. J. Austin, R. Cammi, C. Pomelli, J. W. Ochterski, R. L. Martin, K. Morokuma, V. G. Zakrzewski, G. A. Voth, P. Salvador, J. J. Dannenberg, S. Dapprich, A. D. Daniels, O. Farkas, J. B. Foresman, J. V. Ortiz, J. Cioslowski, D. J. Fox, Gaussian 09, revision A.02; Gaussian, Inc.: Wallingford, CT, 2009. (b) C. Lee, W. Yang and R. G. Parr, *Phys. Rev. B,* 1988, **37**, 785− 789. (c) A. D. Becke, *J. Chem. Phys.,* 1993, **98**, 1372−1377.

15 X. Yi, J. Zhao, J. Sun, S. Guo and H. Zhang, *Dalton Trans.*, 2013, **42**, 2062.

16 O. Kwon, S. Barlow, S. A. Odom, L. Beverina, N. J. Thompson, E. Zojer, J. L. Breedas, S. R Marder, *J. Phys. Chem. A,* 2005, **109**, 9346.